SPE 59295

Waterflood Surveillance and Supervisory Control

Asoke De[1], Dmitriy B. Silin[1], and Tad W. Patzek[1,2,3]

[1]Lawrence Berkeley National Laboratory; [2]University of California at Berkeley; [3]SPE Member, patzek@patzek.berkeley.edu

This paper was prepared for presentation at the 2000 SPE/DOE Improved Oil Recovery Symposium held in Tulsa, Oklahoma, 3–5 April 2000.

Abstract

A successful waterflood depends on the proper operation of individual wells in a pattern, on maintaining the balance between water injection and production over the entire project or field, and on preventing well failures. The problems with waterflood are further aggravated in tight rock, e.g., carbonate, chalk or diatomite, where injector-producer linkages, uncontrolled hydrofracture growth, and water breakthrough in thief layers are often encountered. For optimal operation of a waterflood, it is mandatory that field engineers routinely acquire, store and interpret huge amounts of data to identify potential problems and to address them quickly. The cost of an error can be extreme; failure of only one well may cost more than the entire surveillance-controller system described here. As in preventive health care, it is important to diagnose the problems early and to apply the cure on time. Our solution is to design a multilevel, integrated system of surveillance and control, which acquires and processes waterflood data, and helps field personnel make optimal decisions. Our upper-end systems will rely on the satellite radar interferograms (InSAR) of surface displacement and the new revolutionary micro-electronic mechanical systems (MEMS) sensors. Many intermediate configurations are also possible. In the near future, the next generation of smart, reliable and cheap sensors will revolutionize field operations of small independents and majors alike. We think that the impact of the new technology on the independents will be proportionally larger.

Introduction

Currently there exists no system of automatic or semi-automatic surveillance and control of waterflood projects. Our goal is to create a system that continuously and automatically collects, processes, stores and analyzes data obtained from all the wells and all the sensors, **Figure 1**.

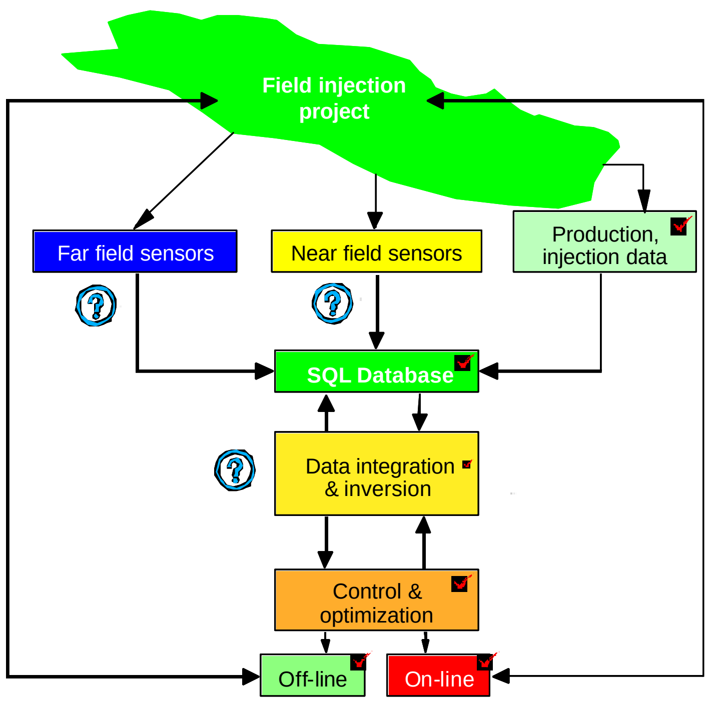

Figure 1 - The proposed field wide system of surveillance and control. The question and check marks denote, respectively, the system parts under development and already developed.

The key idea is to acquire a time-lapse map of the volumetric sweep of injected water by integrating areal sweep from surface displacement and vertical sweep from logs and cross-well images, **Figure 2**. The surface signature must then be integrated with the production and injection data, and must be translated to downhole conditions by using a simple fluid volume balance with an elastoplastic strain model of reservoir rock tied to surface displacement.

The proposed system will operate at different levels of sophistication, depending on the resources of the user. At the simplest level, we can use the traditional field data that are collected by hand. At the most sophisticated level, we can use the Synthetic Aperture Radar interferograms (InSAR) [1-6], and arrays of the new MEMS sensors [7-9], **Figure 3**, to process the information close to real time.

If the field data are sparse and delayed, we can still reconstruct an approximate state of the field by using our surveillance software. The companion controller software then works off-line to enhance waterflood analysis and develop recommendations on the injection rates and pressures. The only hardware required is a PC with our software installed.

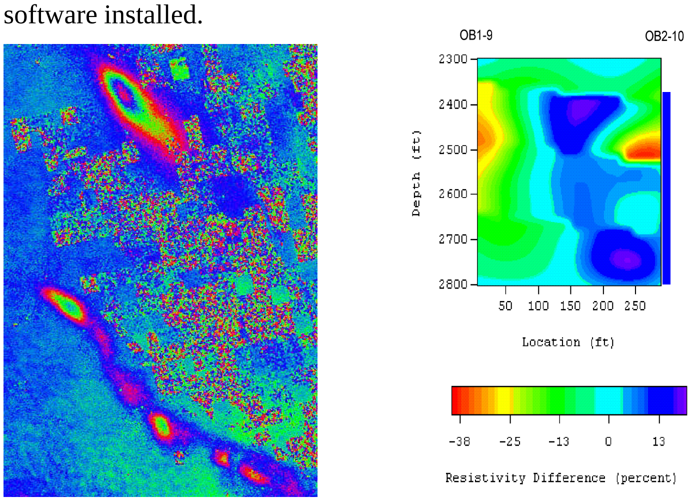

Areal sweep from surface signature

Vertical sweep from Cross-well EM images

Figure 2 - Volumetric sweep is the product of areal sweep from InSAR images or microtiltmeter network and vertical sweep from cross-well logs, EM or seismic. The InSAR image of Lost Hills (north) and Belridge Diatomite was acquired by Atlantis Scientific, Inc. [6]. The dark area in the EM image is the injected water breaking through to a producer. (The EM image is courtesy of EMI, Inc.)

If an SQL database with waterflood operation records exists, similar analyses can be performed by remotely accessing the data. The controller may work either on-line or off-line, depending on the frequency of updates of the database. Therefore, remote connectivity to the database is required.

If the data are automatically collected and stored in a database, the system will diagnose the status of the waterflood on-line, signaling unexpected events in real-time. The controller can now be used on-line in automatic mode. Equipment for automatic data acquisition and on-line connectivity to the database are required. Besides injection-production data, the analysis will be based on the input from InSAR, EM or seismic cross-well images, and arrays of distributed permanent MEMS sensors performing on-line monitoring of pressure, flow rate, temperature, fracture extensions, volumetric sweep, subsidence, etc.

The important features of our existing software are:

- Direct connectivity to remote SQL databases
- Temporal and spatial visualization of field data
- Model-based analysis of primary and waterflood production and injection
- Forecasting of production and injection
- Model-based robust control

The software features an easy to use and intuitive graphical user interface. It communicates dynamically with _any_ SQL database that stores the field data, giving automatic network access to the most current field information. The software allows both static and temporal visualization and model-based analysis of the existing field data, either well-by-well or field-wide. It also features various tools that address the key problems of waterfloods. The software analyzes the nearest-neighbor interactions between producers and water injectors and identifies waterflood response and direct injector-producer coupling. In addition, it provides estimates for the growth of injection hydrofractures from the water injection rate-wellhead pressure data. The fracture growth estimates are crucial for the prevention of catastrophic hydrofracture extensions, reservoir damage and well failures.

Field Examples of InSAR Use

Rapid ground motion over areas of petroleum and gas extraction has been observed worldwide and measured with InSAR [2, 6, 10-19]. In addition, InSAR technology has been used to detect mine collapse, underground explosions and earthquakes [20].

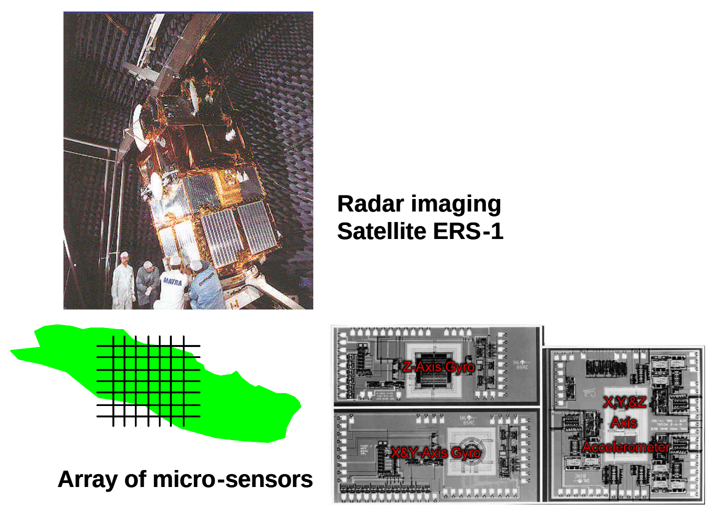

Figure 3 - A pair of radar imaging satellites are the far field sensors, while the 9 mm micro-electronic-mechanical (MEM) chip from Integrated Micro Instruments will be modified and deployed as cheap reliable microtiltmeters in a large surface array.

Lost Hills, CA. As late as mid-1998, preliminary elastic strain modeling [2] in the Lost Hills oilfield indicated a net compaction of 1.7 mm day^{-1} at the center of the subsidence bowl decreasing to 0.6 mm day^{-1} to the south, **Figure 4** and **Figure 5**. That much compaction over a total area 0.8 x 5 km^2 could account for the observed surface subsidence of the 35-

day interferogram. Figure 4 shows that over an 8-month period there was too much subsidence at Lost Hills to preserve image coherency. The modeling demonstrates that the volume change in the reservoir rock, sufficient to cause the observed signal, is roughly $1.5x10^6$ m^3 yr^{-1} (9,400,000 bbl/yr) for the Lost Hills oilfield. The annual damaged pore volume is equal to the cumulative water injection from 100 injectors, injecting continuously at 250 BWPD. (Fewer wells injecting at a higher rate are not necessarily better.) We estimate that the cost of the additional injectors would be about $40,000,000, not counting surface facilities. Because we do not know exactly where the injected water is going, mere infilling will not suffice. Uneven areal sweep may cause massive well failure. With 500 producing wells, a 5% failure rate translates into an annual cost of roughly $10,000,000. A data-driven, field-wide injection and withdrawal control system is therefore desirable and possible at a *lifetime* cost that may be less than the *annual* budget for the replacement of failed wells.

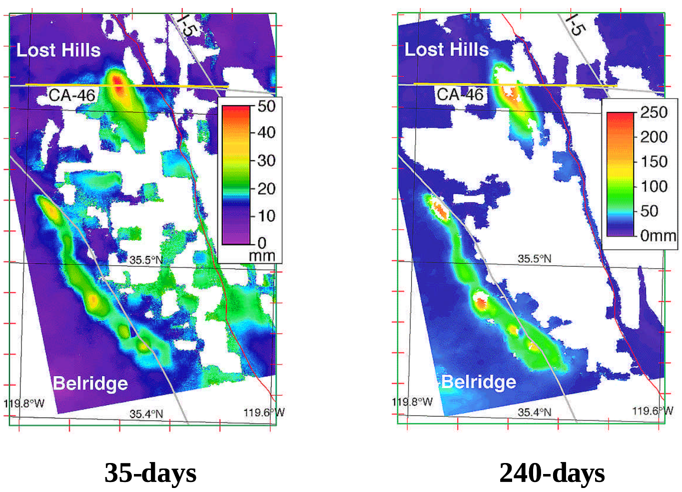

Figure 4 - 35-day and 240-day elapsed InSAR images showing surface displacement in Lost Hills and the Belridge Diatomite. The white areas are decorrelated due to surface plant growth or too much displacement. (From [2])

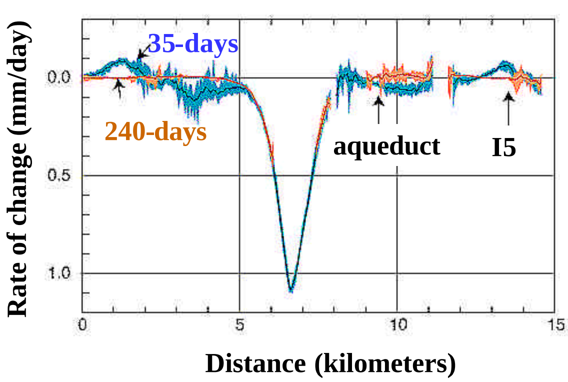

Figure 5 - Rate of surface deformation observed along CA Hwy 46, yellow line in Figure 4. Note that the 240-day interferogram is decorrelated in the middle of the subsidence bowl (From [2]).

In the arid and flat South Belridge and Lost Hills area, where radar coherency can be achieved for periods of months to years, Figure 4, InSAR permits surveillance capability and monitoring of land subsidence at unprecedented spatial detail and costs comparable to conventional surveys. Where large scale, high-density change detection is required, such as in large waterflood projects, InSAR could yield a considerable cost advantage over conventional surveys.

In oilfields prone to large-scale compaction, such as South Belridge and Lost Hills, the high spatial detail of InSAR displacement maps may illuminate the following phenomena:

- Crustal deformations related to greater lateral variability of sediments
- Fault activity
- Transients from infill well drilling and fracturing programs, including fracture azimuth
- Areal distribution of injected water
- The localized effects of individual water injectors and waterflood project well clusters on the global stress field

Many of these features of oilfields under water injection, all of which affect compaction, are now poorly defined and sparsely measured.

Yibal, Oman. Petroleum Development Oman LLC (PDO) has successfully employed InSAR to detect and measure surface subsidence in the Yibal oil and gas field, Sultanate of Oman [4]. This project was initiated in July 1998, in response to an increased frequency of reported minor earth tremors in the vicinity. The cause of the tremors was presumed to be natural tectonic events, or localized subsidence resulting from fluid and gas extraction from the subsurface. It is generally understood that the interior of Oman is not a region characterized by tectonic seismicity.

Hydrocarbon production in Yibal occurs in three geologic formations at different depths [21]. The Khuff reservoir is the deepest (3000 m subsea), and it produces very little oil. Pressure in the Shuaiba reservoir (122 m thick) is maintained by means of water injection; structural faults in this formation are regarded as very permeable and water conductive, therefore it is unlikely that the injection process causes reactivation due to reduced friction along the fault. The Natih gas reservoir is the shallowest; gas production from this interval is ongoing, and reservoir pressure has decreased from 10120 kPa to 7920 kPa.

Based on available information, it is likely that the reported tremors in Yibal are caused by the depletion of the Natih gas reservoir. As hydrocarbon reserves are removed, the host formation will undergo compaction, and dormant subsurface faults may be re-activated. Compaction may lead to a reduction of reservoir porosity, which in turn would affect production levels. Reactivation of faults may compromise the integrity of the reservoir seal, resulting in natural migration of hydrocarbons to other formations or to the surface.

ERS (the European Remote Sensing Satellite) tandem mode data were acquired to derive a high-resolution digital elevation model for removal of topographic phase effects from subsequent interferometric SAR pairs intended for subsidence modeling. Deformation maps were produced using JERS L-band SAR image pairs acquired in 1995/96, over a time period of 440 days, **Figure 6**, and RadarSat fine beam SAR image pairs acquired in 1998, over a time period of 120 days.

Results of the investigation clearly indicate that surface subsidence is occurring in Yibal and that the affected area coincides with a particular geologic formation, which is currently producing Oman's domestic gas supply. Derived subsidence rates are supported by the results of conventional geodetic measurements. However, the effects of tropospheric variations occurring during the SAR acquisition period are suspected to induce significant phase differences between interferometric pairs, which may bias the subsidence model if not adequately compensated [22].

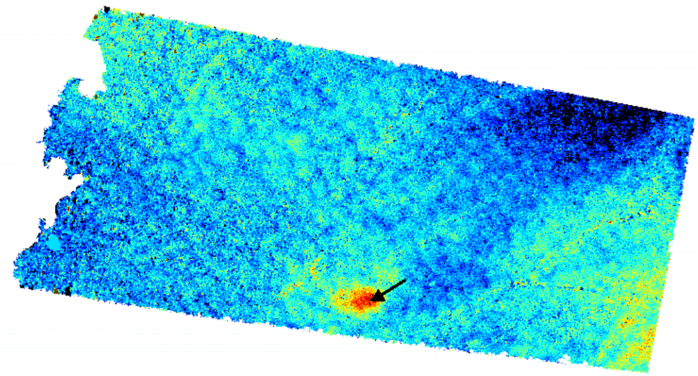

Figure 6 - Deformation map derived from the Jan. 1 1995/Mar. 16 1996 JERS-1 pair. Arrow points to location of maximum deformation (8.4 cm or 6mm/month) ©Atlantis Scientific [4].

Table 1. Methods of Measurement of Surface Displacement [3]

Method	Displacement component	Precision[1] mm	Sample Frequency[2] 1/day	Sample density[3] 1/survey	Survey scale
Borehole extensometry	vertical	0.01-0.1	continuous	1	point
Leveling	vertical	1-10	1-10	10-100	line
GPS	horizontal	5	10-30	10-100	network
GPS	vertical	20	10-30	10-100	network
InSAR	range	10	$>>10^6$	10^5-10^7	map/pixel

[1]Precision that is generally attainable under optimum conditions.
[2]Number of measurements generally attainable in one day under optimum conditions at benchmarks and reference points within the scale of the survey.
[3]Number of measurements generally attainable under optimum conditions to define the distribution and magnitude of land subsidence at the scale of the survey.

Methods of Surface Monitoring

InSAR requires geodetic control to relate indicated changes to stable datum; presently, this is best accomplished using GPS and leveling surveys tied to extensometer sites and/or surface tiltmeters where possible. Coincident ground control can also constrain error of the radar interferometric technique. At the oilfield-scale, the detection precision of surface displacements, **Table 1**, generally attainable by InSAR under optimum conditions (5-10 mm), is comparable to conventional leveling (1-10 mm) and GPS surveys (5-20 mm). The InSAR-detected range changes represent differencing of spatially averaged estimates over the area of a pixel (10-by-10 m or 50-by-50 m) or pixels, whereas measurements derived from conventional surveys result from differencing point measurements. However, given the sparseness of surveyed measurements at the oilfield scale, neither of these conventional techniques can realistically compete with the high spatial detail possible with InSAR at this scale. On the other hand, InSAR cannot supplant borehole extensometry and surface tiltmeters for precise (<0.01-0.1 mm) and continuous measurements of the oilfield compaction at a single location or of the surface motion over a small area.

MEMS Tiltmeters are examples of the new generation of microsensors [8, 9, 23]. The term "Micro-Electro-Mechanical Systems" (MEMS) refers to the technologies and applications of three-dimensional devices with sizes in the micrometer-millimeter range. MEMS devices involve creating controllable mechanical and movable structures using IC technologies. MEMS were born by marrying microelectronics with micromachining. Microelectronics, the production of electronic circuitry on silicon chips, is a very well developed technology. Micromachining is the fabrication of structures and moving parts. These technologies together can deliver perhaps the ultimate sensor system: a completely passive sensor, which is driven and interrogated by a remote control unit. The sensor itself is small but allows for reasonable complexity. Self-packaging for harsh environments is common. Sensitivity and selectivity to the variable to be measured is high. Autocalibration and autoranging are attributes that are very important and enhance system performance by large margins. In the end, there is the issue of cost effectiveness that demands a low-cost high-performance system.

The inherent size, weight, power consumption, and cost advantages of MEMS can be reinforced by integrating circuitry with the micromachined silicon sensing-element [8]. Batch fabrication utilizing standard VLSI compatible surface micromachining techniques can virtually eliminate the need for a multitude of discrete components on large printed circuit boards, thereby providing extreme miniaturization and improved reliability. The same CMOS switched capacitor technology prevalent in the highest performance 20-24 bit sigma-delta analog-to-digital converters can be used to design precision MEMS sensors. Placing interface electronics, signal processing, and analog-to-digital conversion on chip allows improved signal-to-noise performance [9], offset cancellation for bias stability, force balancing for scale factor stability, and noise immune digital output. Additional features might include digital filtering, bus communication, and microprocessor decision-making. In the future, integration may come to apply to more than just circuitry. The mechanical sensors themselves may be integrated together to form entire monolithic microsystems.

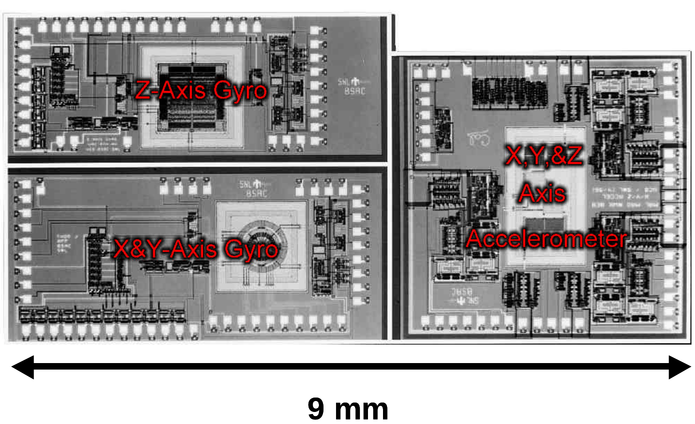

Figure 7 – A full six-degree-of-freedom inertial navigation unit designed by IMI researchers while at U.C. Berkeley and fabricated by Sandia National Laboratories, courtesy of T. Roessig, IMI.

Figure 7 shows a micro-inertial measurement unit fabricated by Sandia National Laboratories and designed by Integrated Micro Instruments (IMI) team members while still affiliated with the Berkeley Sensor & Actuator Center (BSAC) [8]. The sensors required for measurement of rotation and acceleration in all three orthogonal directions, interface circuitry, signal processing, and even analog-to-digital conversion are all integrated on a single 9-by-5 mm silicon chip. The sensors are aligned photo-lithographically on a single flat wafer. Circuit integration clearly allows extreme miniaturization because only a few passive external components are needed. A redesigned version of this chip will become the new microtiltmeter. The current chip roughly has a 100 $mg/\sqrt{\text{Hz}}$ noise-floor, whereas the new Silicon-On-Insulator SOI-MEMS chip will have a 5 $mg/\sqrt{\text{Hz}}$ noise-floor (g is the acceleration of gravity).

The preliminary specifications for the microtiltmeter chip are:

- It can function at temperatures from -40^{0}C to 140^{0}C, but the temperature cannot change during use if reasonable resolution is to be maintained
- The device will survive a 20g vibration and 1000g shocks for 11 ms, but it will not measure during the shock events
- The output power is not an issue
- The size will be less than one inch on a side for the package

Integrated Surveillance/Control Software

In most waterflood projects, the production and injection data are collected sporadically, which may result in failure to detect injection fracture extensions as they happen. However, the signature of a fracture extension remains and can be detected from the data collected later. The quality of data is also questionable at times, which may complicate the analysis. Pattern-wide or a section-wide analysis can help in such cases by smoothing out some of the local errors.

Even sufficiently reliable data are often spread out over different databases, and need to be accessed and processed by several different software packages for a meaningful analysis of a waterflood. This data mining and integration can be a significant burden on the reservoir engineers' time, which could be better utilized; hence, there is a definite need for an integrated waterflood surveillance system. Our particular implementation of such a system is called the Waterflood Analyzer.

Some of the important features of the Analyzer are:

- Remote, dynamic connection to SQL databases
- Temporal visualization of field data
- Sophisticated analysis tools for oil, water, and gas production
- Wavelet-based analysis of injector-producer interactions

– Field-wide production and injection forecasting
– Suggestions for operating policy changes that ought to be made in order to improve the waterflood performance (supervisory control)

The software features an easy to use and intuitive graphical user interface. It communicates dynamically with *any* SQL database that stores the field data, giving automatic network access to the most current field information. The software allows both static and temporal visualization and model-based analysis of the existing field data, either well-by-well or field-wide. The Analyzer also features various tools that address the key issues in waterflooding. The software analyzes the nearest-neighbor interactions between producers and water injectors, and identifies waterflood response and direct injector-producer coupling. In addition, it provides estimates of the growth of injection hydrofractures from the water injection rate-wellhead pressure data. These estimates are crucial in the prevention of catastrophic hydrofracture extensions, reservoir damage and well failures.

In the following sections, we first present the various types of field data that drives the surveillance system and introduce you to the various features of the Analyzer. Finally, we discuss the supervisory control capabilities of the Analyzer.

Field Data Inputs. The Analyzer is data-driven; hence, the quality of surveillance, analysis and control that it can achieve are intimately related to the nature of field data available. The types of field data inputs are:

- Direct measurements (injection pressure, injection rate, production data)
- Remote sensing data of reservoir state, e.g., InSAR, surface and vertical arrays of traditional and micro tiltmeters, EM, cross-well seismic images, resistivity logs, C/O logs (GST - Gamma Spectroscopy Tool), etc.
- State of injection hydrofractures (injector wellhead pulsing)
- Geologic and petrophysical properties of the formation (layering, faults, porosity and permeability maps, fluid saturations, fluid properties)

Based on the available data, the Analyzer can create a three-dimensional map of the volumetric distribution of the injected fluid and relate it to well failure rate and waterflood performance.

Direct measurements of injection and production rates constitute the minimal input data set the Analyzer needs for the creation of such a map. The production/injection data are readily available since all companies collect them regularly.

Injector wellhead-pulsing can provide a direct measure of the state of the injection hydrofracture, as well as help detect catastrophic hydrofracture extensions.

An integrated data inversion engine generates the map at various degrees of sophistication, depending on the available data:

1. *Least* — based solely on the injection/production data. The map is created through a spatial-temporal correlation of the data. The inversion of the injection rate - injection pressure data provides indirect measure of the injection hydrofracture state, which is used to refine the map.
2. *Intermediate* — based on additional data from wellhead pulse tests. Instead of using indirect estimates of hydrofracture state, direct hydrofracture state estimates can be used by the inversion engine, along with the injection/production data.
3. *Full* — based on the integration of surface motion, well logs, geology, etc. (not implemented yet).

Model-based analysis tools and the inversion engine constitute the core of the Analyzer.

Analyzer Features. The Analyzer tools can be broadly classified as Database tools, Visualization and Analysis tools, and Supervisory Control tools. The Analysis tools available to the user depends on the mode of analysis, namely,

– Well-by-well
– Several wells in a section
– Single well and its nearest neighbors
– Section-wide or field-wide analysis

These tools are accessible through the Main Window of the Analyzer. The first step is to select the desired field section from either the internal or the external database. Once the section is selected, a clickable map of the wells in that section is displayed in the main window, **Figure 8**, and the appropriate Analysis tools become available.

Database tools. Database tools perform the task of data extraction, integration and storage. The Analyzer can directly access the current data in the corporate SQL databases, e.g., Oracle, which can be located either locally or remotely. A database setup program allows us to link the internal variables of the Analyzer to the appropriate data fields in the corporate SQL databases. Once the links are set up, Analyzer can directly extract required data from the databases through SQL queries. Optionally, an internal database can be set up by extracting relevant data from the corporate databases and storing these data in binary format. Creating an internal database leads to significant increase in the speed of operation. The appropriate database can be chosen through the *Select* menu option of the Main Window.

The Database tools work equally well with *Microsoft Access*, which is part of the Microsoft Office suite. A set of offline tools can also be used to parse data in text or spreadsheet format and create appropriate *Access* databases.

Visualization and Analysis. The Visualization and Analysis tools can be broadly classified into static and temporal analysis tools. While the static tools can be used for all the modes of analysis mentioned earlier, the temporal tools can only be used for section-wide analysis. We now briefly describe these tools in relation to the four modes of analysis.

Well-by-well Analysis. We can perform two types of analyses on a well-by-well basis: the analysis of the historical well production (or injection) data and the response of a producer to waterflooding. An additional tool for the estimation of the hydrofracture growth, by inversion of injection and pressure data, is available for the injectors, **Figure 9**.

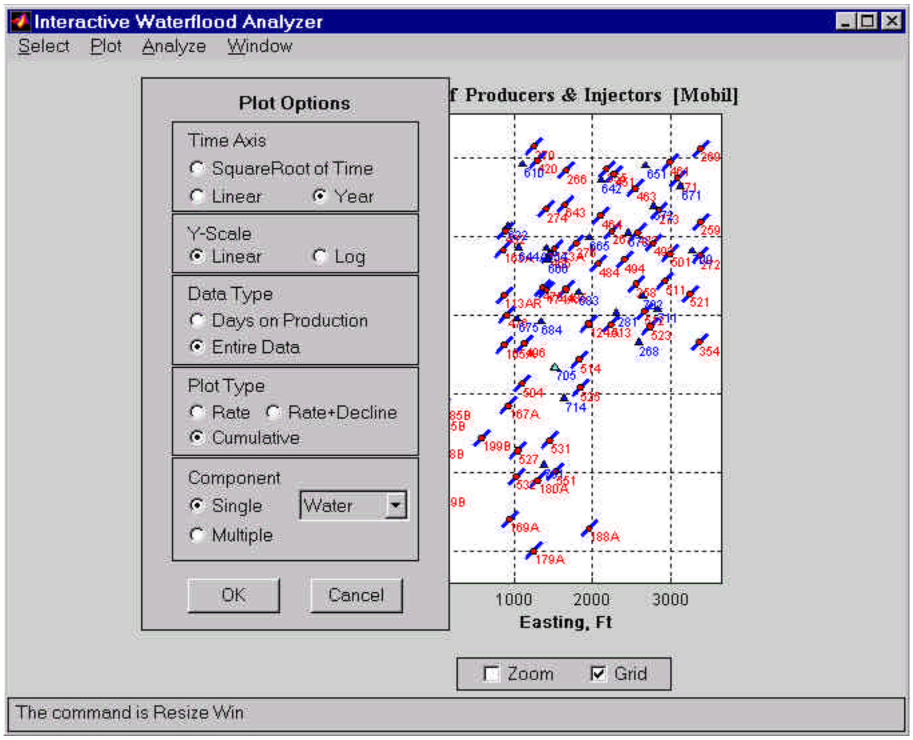

Figure 8 - The Main Window of the Analyzer showing the clickable map of the wells in a section and the Plot options window that pops up when a well is selected.

The well-by-well analysis of the historical data can be performed through the clickable section map displayed in the Main Window, or by using the Interactive Plot tool. Both tools allow us to display the entire production (or injection) data of the well as cumulative volumes or volumetric rates. In addition, we can plot the decline curve for the production data.

The response of a producer to waterflooding can be analyzed using Linkage Analysis tool. The tool is based upon wavelet analysis of the production data for the detection of waterflood response, cross-correlation of the water injection in neighboring injectors, and the oil and water production in the producer, **Figure 10** and **Figure 11**.

Multiple Wells. The Interactive Plot tool allows us to analyze multiple producers (or injectors) in a section by choosing them from a pull-down list of the wells. We can also add wells one at a time while holding on to the previously selected wells. A small map located in the top right corner of the Interactive Plot window shows the spatial relationship between the wells.

Neighbors. The Nearest Neighbor Analysis tool lets us examine a well and its nearest neighbors. There are four options: 1) producer and its neighboring producers, 2) injector and its neighboring injectors, 3) producer and its neighboring injectors, and 4) injector and its neighboring producers. The nearest neighbor analysis helps us identify any anomalous behavior in a small region of the section and potential producer-injector linkage. An optimal triangulation algorithm is used to detect the nearest neighbors. An example of picking the “same sex” neighbors of a producer is shown in

Figure 12. In **Figure 13**, the relative performance of the neighboring producers is compared.

Entire Field Analysis. The Section-wide Analysis tools let us examine, among others, the average productivity and injectivity of a section, its average waterflood response, as well as the temporal evolution of the field. The Analyzer displays the average oil, water or gas productivity of a section as a two-dimensional filled contour plots of the production slopes, **Figure 14**. In these plots, blue represents low productivity regions and dark red represents high productivity regions. Similar contour plots can be obtained for the water injectivity. We can also obtain a contour plot for the waterflood response of the section. In addition, the Analyzer can generate a three-dimensional surface plot showing the relationship between water injection and waterflood response for the section, **Figure 15**. The height of the surface represents

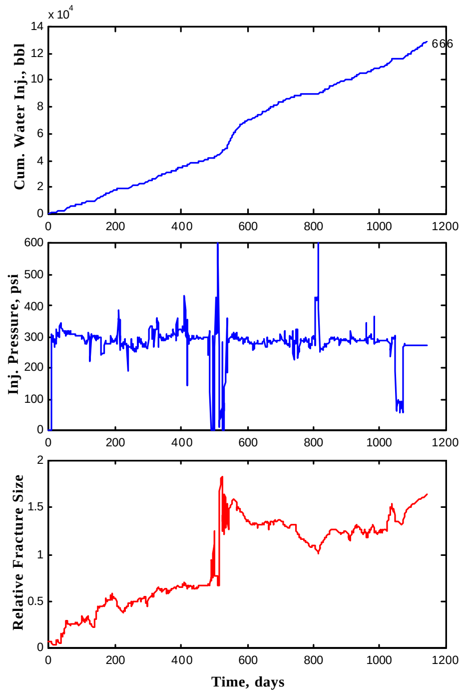

Figure 9 - Injection hydrofracture size estimation from injection pressure and injection volume data for a given well. An uncontrolled pressure fluctuation led to an approximate doubling of the fracture size.

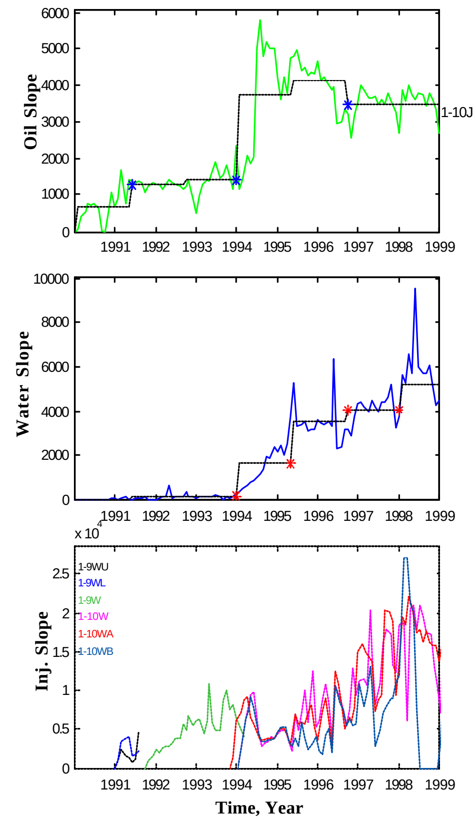

Figure 10 – Automatic detection of injection and production slopes and cross-correlation of these slopes for the neighboring wells.

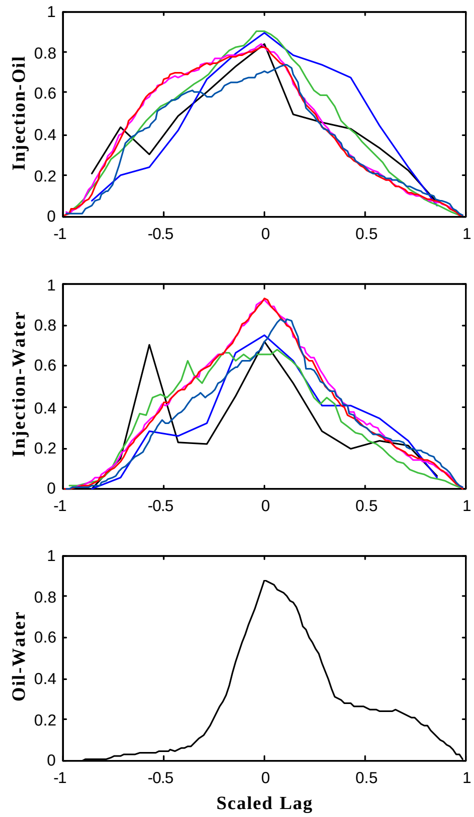

Figure 11 - Identification of individual well waterflood responses through wavelet analysis.

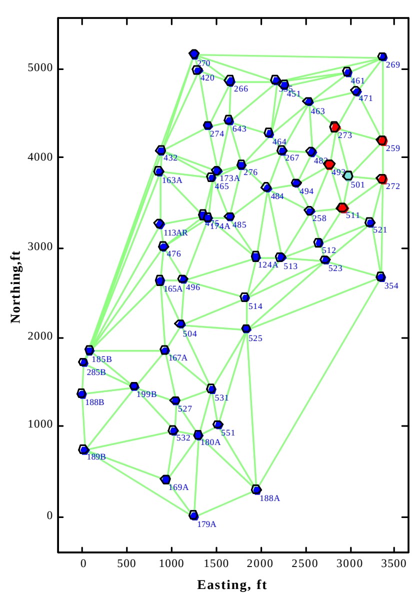

Figure 12 – By clicking on a well (here 501), its nearest neighbors of are found automatically through a Voronoi tessellation of the field-wide well layout.

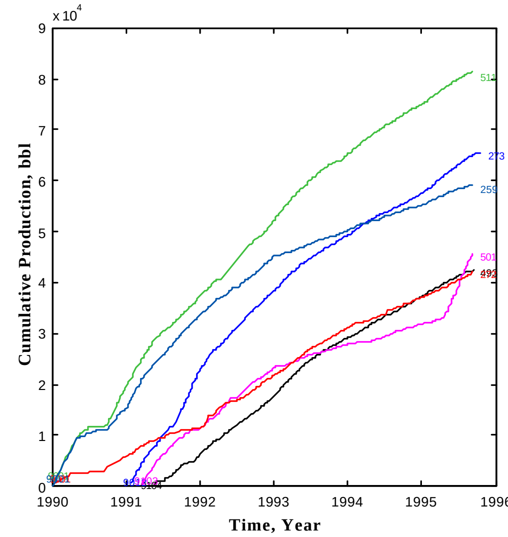

Figure 13 – The cumulative production (or injection) of all neighbors of the well picked in Figure 12 is automatically displayed.

the average injection slope and the surface colors provide a measure of waterflood response.

Animation. The Animation tool lets us examine the production and waterflood response over time. As in the case of static plots, either we can have animation of two-dimensional contour plots or three-dimensional surface plots. Each frame of the movie is a snapshot in time of the production and /or injection rates.

Another useful tool is the Domain Plot, which generates either a producer-centered or an injector-centered Voronoi map for the wells in a section. The map identifies the domain of influence of a given injector or producer and helps assess the optimality of well placements.

Forecasting. The Forecasting Tool allows us to forecast individual well production/injection, but also production/injection by patterns or by sections, under prevailing conditions. In addition, the Forecasting Tool allows us to investigate interactively under several different scenarios, where infill or new producers could be added. Finally, we can perform injection and production forecasting based on the fluid distribution map.

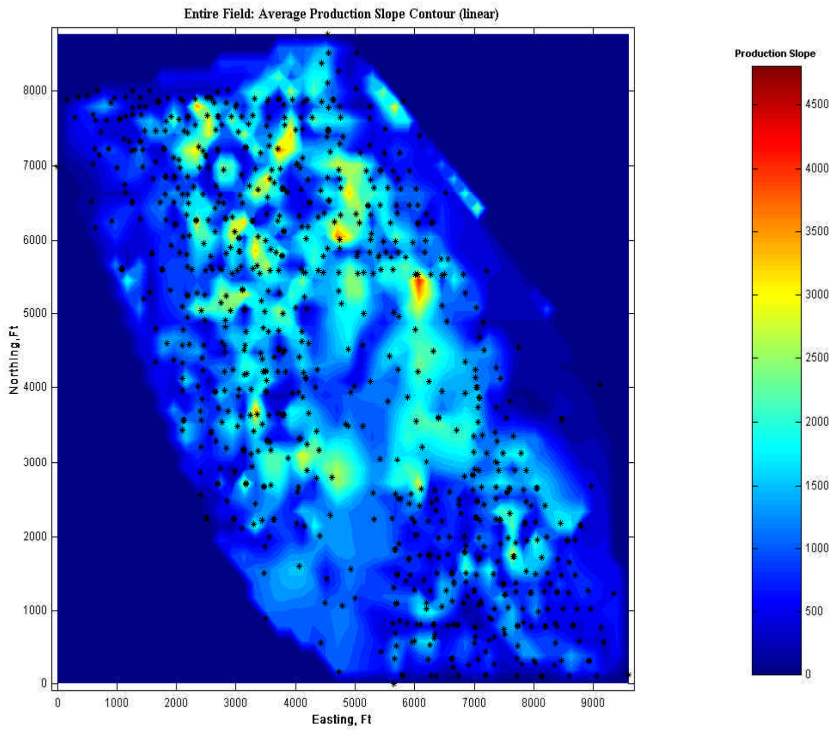

Figure 14 - Contour map of the average oil productivity spanning several properties belonging to different companies. The brightest areas have the highest productivity.

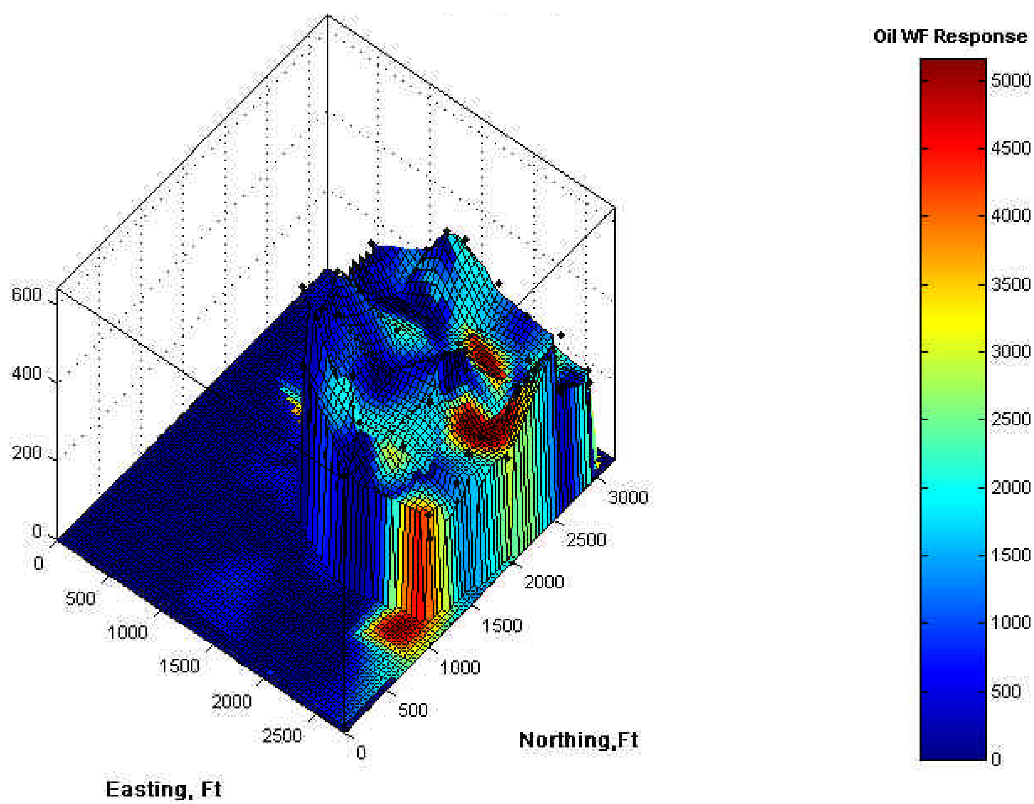

Figure 15 – A single frame from and animated correlation between water injection-rates (height of the surface) an oil responses (color) in a waterflood section. Note that the areas that receive less water have the highest oil production response (brightest colors).

Supervisory Control. The Supervisory Control Tool operates in two modes: semi-automatic and automatic. In the semi-automatic mode, it helps reservoir engineers identify problematic wells, flags injectors undergoing extensive hydrofracture extension, and suggests modifications, if any, which need to be made in the operating conditions. In the automatic mode, contingent on the availability of control hardware for injectors, the supervisory control tool automatically modifies the operation of injectors, based on the recommendations of the Analyzer.

The Control Tool utilizes analysis of the data. At the same time, it supplies data back to the Analyzer. Therefore, both parts of the system are mutually connected and feed each other. Reflecting our approach, the control tool is hierarchical and may be implemented at several levels of automation.

At the highest level, the decisions are made on a field scale, based on the global waterflood analysis. For example, in some areas water injection may need to be increased because analysis of InSAR images or microtiltmeter data indicates considerable formation subsidence. In other areas, the injection may need to be decreased due to the increase of water cut or presence of thief layers signaled by the Analyzer.

At a lower level, the decisions based on the field-scale analysis are implemented at each individual injector. The injection is regulated by increasing or decreasing the injection pressure through adjusting the valve opening. This mode of operation is rather delicate, especially if the injection rate must be changed to a new value. Trial and error approach is inaccurate and may take considerable time. Excessive injection pressure may lead to a substantial fracture extension and may necessitate reviewing the waterflood policy in a larger area, not only in the neighborhood of the fractured injector.

In order to achieve our objectives, the Controller is model-based and accounts for the changing injection conditions. Our controller concept is based on the model of injection through a vertically fractured injector. As demonstrated in previous papers [24, 25], the current instantaneous injection rate depends not only on the current wellhead pressure and on the current fracture size, but it depends on the entire history of injection. Consequently, the injection pressure to be applied now also depends on the history of injection, which is calculated from optimal control theory methods. The controller has three input parameters: the injection rate, the injection pressure and the fracture size. All three are stored as arrays of measurements performed on regular basis. The objective of control is to adjust the injection pressure in such a way that the injection rate is as close as possible to the prescribed value [26, 27].

By analyzing the input data, the Controller outputs the injection pressure to be applied. Knowing the right injection pressure, the injection well valves can be adjusted either manually or automatically, depending on the level of automation of the system.

The same injection model can be used to estimate the effective fracture area. Indeed, a model-based estimate of the effective area is more appropriate as the Controller input than the idealized geometric fracture area. Passing this estimate to the controller input makes it almost a closed-loop device. We say "almost" because as we noted earlier, the optimal injection pressure depends on an array of historical inputs, not just on the instantaneous measurements; therefore, it cannot be generated by a genuine closed loop feedback control.

Our model assumes a layered formation with substantial heterogeneity between layers [27]. Therefore, it is possible that the injected fluid flows in a thin high-permeable zone. If the injection rate under the optimal injection pressure considerably exceeds the target rate, then either it is a signal that such layers do exist or the fracture has experienced an extension event. The latter one can be verified by independent measurements, e.g. using micro-tiltmeters or high-resolution satellite radar images, or hydraulic impedance tests [28]. If the fracture extension is not confirmed, then presence of a thief layer is proven. Thus, the controller can also be used as a monitoring device, which signals such an event before a link to a neighboring producer has been established.

Conclusions

Progress in space and micro-electronic-mechanical technology has made it possible to control the entire waterflood projects viewed as complex, nonlinear and interacting systems. In this paper, we have summarized some of the new exciting technology in imaging motion of the ground surface from space using the Synthetic Aperture Radar interferograms (InSAR) and Micro-Electronic-Mechanical Systems (MEMS) accelerometers that may be used as tiltmeters. We have outlined the main features of our process-driven, flexible system for surveillance and supervisory control of waterfloods. The system is data-driven and can be implemented at different levels of sophistication, depending on the nature of available data. Among others, our system:

- Provides a uniform SQL-based interface for data access, storage, and integration
- Allows remote Web access of data
- Allows static and temporal visualization of field data, either on a well-by-well basis, or on a field-wide basis
- Analyzes and flags potential injector-producer linkages
- Provides estimates of injection hydrofracture growth
- Performs production and injection forecasting
- Analyzes the optimality of well placements
- Works as a supervisory control system at varying levels of sophistication

Acknowledgements

We would like to thank Chevron and Aera Energy for their enthusiastic support of this project, in cash and in-kind. Dr. Robert Lynch of Atlantis Scientific, Inc., has provided the satellite InSAR images and information on Lost Hills, South Belridge, and the Yibal oilfield experiment. Dr. Trey Roessig of Integrated Micro Instruments (IMI) provided the MEMS accelerometer chip images and extensive information. Both Atlantis Scientific and IMI will be our partners in the next stage of this project to be funded in parts by DOE and the Industry. Dr. Eric Fielding of NASA offered helpful comments, Lost Hills images, and future collaboration. This work was partially sponsored by the DOE ORT Partnership and ACTI under Contract DE-ACO3-76FS0098 to the Lawrence National Laboratory of the University of California. Partial support was also provided by gifts from Aera Energy, Chevron and Mobil to UC Oil, Berkeley.

References

1. Gabriel, A. K., Goldstein, R. M., and Zebker, H. A., *Mapping small changes over large areas: differential radar interferometry*. J. Geophysical Research, 1989. **94**(B7): p. 9183-9291.
2. Fielding, E. J., Blom, R. G., and Goldstein, R. M., *Rapid subsidence over oil fields measured by SAR interferometry*. Geophysical Research Letters, 1998. **25**(17): p. 3215-3218.
3. Galloway, L., Hudnut, K. W., Ingebritsen, S. E., Phillips, S. P., Peltzer, G., Rogez, and Rosen, P. A., *Detection of aquifer system compaction and land subsidence using interferometric synthetic aperture radar, Antelope Valley, Mojave Desert, California*. Water Resources Research, 1998. **34**(10): p. 2573-2585.
4. Tuttle, M., Ehrismann, J. and Hulshof, B. *Detection and Monitoring of Surface Subsidence Using Synthetic Aperture Radar Interferometry in the Yibal Oilfield, Sultanate of Oman*. in *ERIM's Thirteenth International Conference on Applied Geologic Remote Sensing*. 1999. Vancouver, B.C.
5. van der Kooij, M., van Halsema, D., Groenewoud, W., Ambrosius, B. A. C., Mets, G. J., Overgaauw, B., and Visser, P. N. A. M., *Satellite radar measurements for land subsidence detection*, in *Proceedings in Land Subsidence*, F.B.J. Barends, and Schröder, F. H., Editor. 1995, Balkema: Rotterdam.
6. van der Kooij, M., *Land Subsidence Measurements at the Belridge Oil Fields from ERS InSAR Data*, . 1997, Atlantis Scientific, Inc.: Nepean, Ontario, Canada.
7. Guckel, H., *Surface micromachined physical sensors*. Sensors and Materials, 1993. **4**(5): p. 251-264.
8. Juneau, T.N., Lemkin, M. A., Roessig, T. A., Clark, W. A., Howe, R. T., Bustillo, J. M., Brosnihan, T. J., and Pisano, A. P. *Commercialization of Precision Inertial Sensors with Integrated Signal Conditioning*. in *Sensors Expo 98*. 1998.
9. Lemkin, M. A., Juneau, T. N., Clark, W. A., Roessig, T. A., and Brosnihan, T. J. *A low-noise digital accelerometer using integrated SOI-MEMS technology*. in *Transducers '99*. 1999. Sendai, Japan.
10. Bowersox, J. R., and Shore, R. A., *Reservoir compaction of the Belridge Diatomite and surface subsidence, South Belridge Field, Kern County, California*. AAPG Bulletin, 1990. **74**(5): p. 616.
11. Colazas, X.C., and Strehle, R. W., *Subsidence in the Wilmington oil field, Long Beach, California, USA*, in *Developments in Petroleum Science, 41, Subsidence due to fluid withdrawal*, G.V. Chilingarian, and Donaldson, E. C., Editor. 1995, Elsevier Science: Amsterdam. p. 285-334.
12. de Rouffignac, E., and Bondor, P.L., *Land subsidence and well failure in the Belridge diatomite oil field, Kern county, California. Part I. Experiments, model and verification*, in *Land Subsidence (Proceedings of the Fifth International Symposium on Land Subsidence)*, F.B.J. Barends, Brouwer, F. J. J. , and Schröder, F. H., Editor. 1995, IAHS Publ.: The Hague. p. 61-68.
13. Doornhof, D., *Surface subsidence in The Netherlands: the Groningen gas field*. Geologie en Mijnbouw, 1992. **71**: p. 119-130.
14. Finol, A., and Sancevic, Z. A., *Subsidence in Venezuela*, in *Developments in Petroleum Science, 41, Subsidence due to fluid withdrawal*, G.V. Chilingarian, and Donaldson, E. C., Editor. 1995, Elsevier Science: Amsterdam. p. 337-370.
15. Holzer, T., Bluntzer, R. L., *Land subsidence near oil and gas fields, Houston, Texas*. Ground Water, 1984. **22**: p. 450-59.
16. Pratt, W.E., and Johnson, D. W., *Local subsidence of the Goose Creek oil field*. J. of Geology, 1926. **34**(7, Part 1): p. 577-590.
17. Sharp, J. M., Jr., and Hill, D. W., *Land subsidence along the northeastern Texas Gulf coast: Effects of deep hydrocarbon production*. Environmental Geology, 1995. **25**(3): p. 181-191.
18. van Hasselt, J.P., *Reservoir compaction and surface subsidence resulting from oil and gas production: a review of theoretical and experimental research approaches*. Geologie en Mijnbouw, 1992. **71**: p. 107-118.
19. Zaman, M.M., Abdulraheem, A., and Roegiers, J.-C., *Reservoir compaction and surface subsidence in the North Sea Ekofisk field*, in *Developments in Petroleum Science, 41, Subsidence due to fluid withdrawal*, G.V. Chilingarian, and Donaldson, E. C.,

Editor. 1995, Elsevier Science: Amsterdam. p. 373-419.

20. Foxhall, W., Sweeney, J. J., and Walter, W. R., *Identification of mine collapses, explosions and earthquakes using InSAR: A preliminary Investigation*, 1998, Lawrence Livermore National Laboratory: Livermore. p. 16.

21. Alsharhan, A.S., and Nairn, A. E. M., *Sedimentary Basins and Petroleum Geology of the Middle East*. 1997, Amsterdam: Elsevier Science.

22. Goldstein, R., *Atmospheric limitations to repeat-track radar interferometry*. Geophysical Research Letters, 1995. **22**(18): p. 2517-2520.

23. Guckel, H., *Micromechanisms*. Philosophical Transactions of the Royal Society: Physical Sciences and Engineering, Series A, 1995(1703): p. 355-66.

24. Patzek, T.W., and Silin, D. B. *SPE 39698: Control of Fluid Injection into a Low-Permeability Rock. 1. Hydrofracture Growth*, in *SPE/DOE Improved Oil Recovery Symposium*. 1998. Tulsa, OK: SPE.

25. Patzek, T.W., and Silin, D. B., *Control of Fluid Injection into a Low-Permeability Rock. 1 - Hydrofracture Growth*. Transport in Porous Media, 1999. **submitted**.

26. Silin, D.B., and Patzek, T.W., *Control of Fluid Injection into a Low-Permeability Rock. 2 - Optimal Control*. Transport in Porous Media, 1999. **submitted**.

27. Silin, D.B., and Patzek, T. W. *SPE 59300: Control of Water Injection into a Layered Formation*. in *2000 SPE/DOE Improved Oil Recovery Symposium*. 2000. Tulsa, OK.

28. Patzek, T.W., and De, A., *Lossy Transmission Line Model of Hydrofractured Well Dynamics*. Int. J. Petr. Eng., 1999. **In print**.